Numerical Simulation of Air Cavity with Water Waves

Yuxi Huang*[1], Xin Wang[1], Arun Dev[1], and Dominic A. Hudson[2]

[1]Newcastle University in Singapore, Singapore
[2]University of Southampton, Southampton, UK
*y.huang51@newcastle.ac.uk

1 Introduction to Air Lubrication Systems

Air Lubrication Systems (ALS) are installations which forces air bubbles out from flat bottom of ships underway. These bubbles coalesces or break up as they travel along hull, forming a layer of bubbly flow. Buoyancy forces these bubbles to travel along boundary layer of hull, resulting in ship experiencing drag reduction. This reduction is achieved through changing interface interaction from that of hull-water to hull-air.

Past studies on ALS focused on drag reduction effects and topology [2] [3] with limited emphasis on effects of waves. Cavity behaviours under influence of free surface closely mimics how air lubrication will work on actual ships and is an important component in estimating drag reductions. This study sets to understand how simple free surface movements affect cavity topology and its drag reduction.

2 Methodology

Symmetrical model of Kriso Container Ship (KCS) with scale factor of 31.6 and L_{PP} of 7.27m was utilised for simulations. Virtual towing tank is of 36m length × 9m breadth × 27m height. Origin of Cartesian coordinates for flow domain was set at rudder stem. A 5mm diameter air injection nozzle was placed 4.6m upstream of rudder stem on flat bottom of ship. Trimmed cell mesher with $y^+ = 30$ prism layer was utilised for flow domain discretization. Figure 1 shows the boundary conditions and meshing of domain with sectional views detailing mesh near ship and free surface.

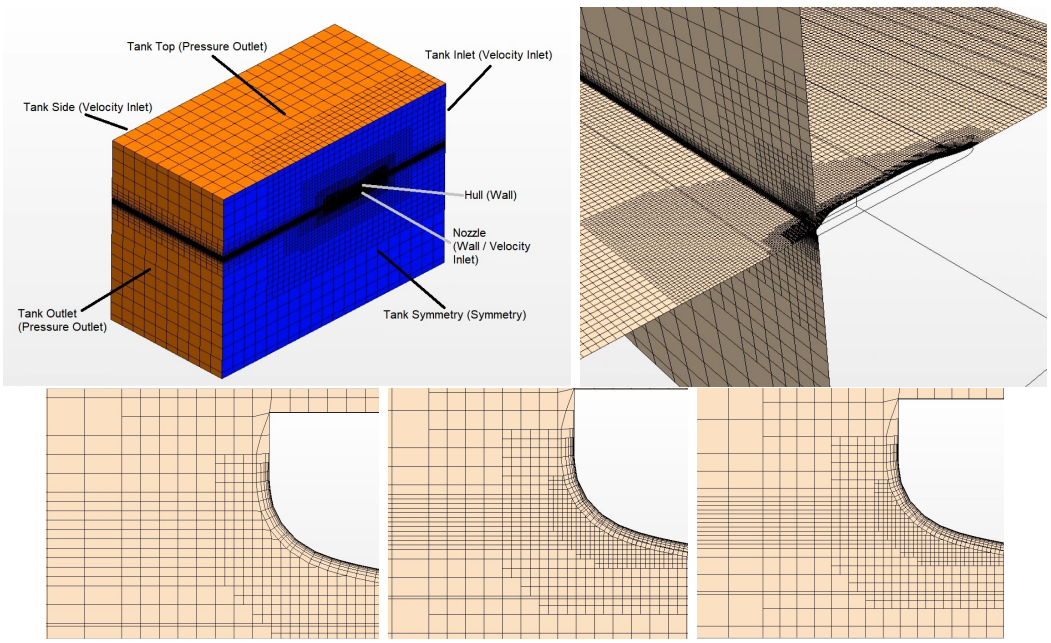

Figure 1: Boundary conditions and meshing details of flow domain with free surface refinement. Bottom left to right: flat waves, wave height = 0.06m and wave height = 0.12m.

Freestream velocity (U_∞) is based on Froude number between 0.1949 and 0.2599 for parametric studies. Additional cases for U_∞=$2ms^{-1}$ and $3ms^{-1}$ were utilised for validation. 5^{th} order waves were defined by their wave height (H_W) and wavelength (λ) normalized over L_{PP} where $\lambda/L_{PP} = 1$. Simulation conditions are described in Table 1.

Freestream Speed (U_∞)	$1.647ms^{-1}$, $1.922ms^{-1}$, $2ms^{-1}$, $2.196ms^{-1}$, $3ms^{-1}$
Air Flux (Q)	$0.002m^3s^{-1}$, $0.0025m^3s^{-1}$
Air Properties	Ideal gas (IG), constant density (CD)
Wave Height (H_W)	Calm, 0.06m, 0.12m
Ship Movement from Fluid-Body Interaction	Heave/sinkage and pitch/trim, fixed

Table 1: Test case matrix

Volume of Fluid (VoF) model and Realizable k-epsilon ($Rk\varepsilon$) model were used to define multiphase and turbulence respectively. Time step sizes of 0.01s & 0.02s were used for simulations with 5^{th} order waves and calm water respectively, chosen based on ITTC guidelines [1]. Simulations were of transient unsteady state and assumed to settle into a quasi-steady state. As such, temporal discretisation were of first order with other discretisation maintained at second order upwind.

3 Results and Discussions

3.1 Sweep Angle (φ)

Sweep angles (φ) of air cavities were drawn from the maximum transverse displacement of interface. A downstream length of approximately 1m from nozzle was used to limit topology to flat bottom of ship. Cavity contours were compared to experimental data [3]. Figure 2 shows these simulated cavity contours beside experimental results.

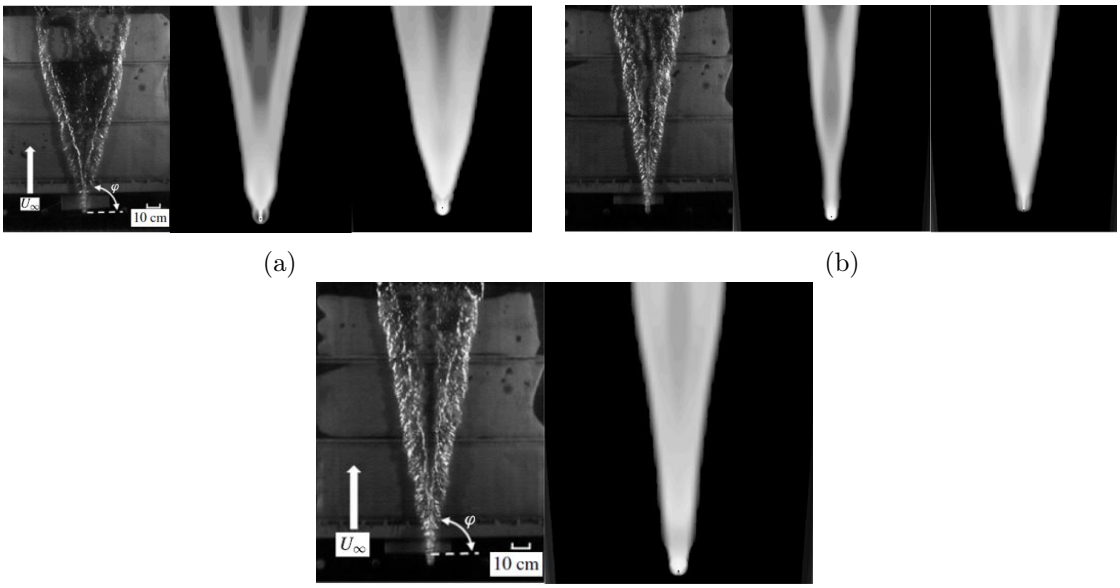

Figure 2: Comparison of experimental photos [3] and simulations with $Q = 2 \times 10^{-3}m^3s^{-1}$ at $U_\infty = 2ms^{-1}$ (a) and $3ms^{-1}$ (b) . Arranged from left to right: Experiment, constant density and ideal gas. $Q = 2.5 \times 10^{-3}m^3s^{-1}$ at $U_\infty = 3ms^{-1}$ (c), experiment (left) and constant density gas (right).

Measurements of angles drawn from max transverse displacement averaged over 1 second upon stable injection of air flux are shown in Tables 2, 3 and 4. Table 2 compares the effects of gas properties to experimental data. Table 3 compares the effects of trim and sinkage on sweep angle. Table 4 compares the effects of gas properties under freestream velocities used for parametric studies.

U_∞	Air Flux	Gas Properties	Sweep angle	% Difference
$2ms^{-1}$	$2 \times 10^{-3}m^3s^{-1}$	N.A	74.2°	Experiment
		CD	78.99°	6.45% to Exp.
		IG	77.99°	5.11% to Exp.
	$2 \times 10^{-3}m^3s^{-1}$	N.A	79.9°	Experiment
		CD	84.58°	5.86% to Exp.
		IG	83.11°	4.02% to Exp.
$3ms^{-1}$	$2.5 \times 10^{-3}m^3s^{-1}$	N.A	80.3°	Experiment
		CD	83.12°	3.52% to Exp.

Table 2: Effects of ideal gas or constant density gas on sweep angle without trim or sinkage.

U_∞	Air Flux	Pitch & Heave	Sweep angle	% Difference
$2ms^{-1}$	$2 \times 10^{-3}m^3s^{-1}$	No	78.99°	0.60%
		Yes	79.46°	
$3ms^{-1}$	$2 \times 10^{-3}m^3s^{-1}$	No	84.58°	0.1%
		Yes	84.50°	
	$2.5 \times 10^{-3}m^3s^{-1}$	No	83.12°	1.32%
		Yes	84.22°	

Table 3: Effects of trim and sinkage on sweep angle.

$U_\infty(Fr)$	Air Flux	Sweep Angle (CD)	Sweep angle (IG)	% Difference
$1.647ms^{-1}$	$2 \times 10^{-3}m^3s^{-1}$	75.13°	73.89°	1.68%
(0.1949)	$2.5 \times 10^{-3}m^3s^{-1}$	74.34°	72.73°	2.21%
$1.922ms^{-1}$	$2 \times 10^{-3}m^3s^{-1}$	78.32°	77.02°	1.68%
(0.2274)	$2.5 \times 10^{-3}m^3s^{-1}$	78.30°	75.60°	3.58%
$2.196ms^{-1}$	$2 \times 10^{-3}m^3s^{-1}$	80.05°	79.14°	1.15%
(0.2599)	$2.5 \times 10^{-3}m^3s^{-1}$	79.54°	77.76°	2.29%

Table 4: Effects of ideal gas or constant density gas on sweep angle with trim or sinkage for parametric studies.

The usage of VoF model for ALS incorporating free surface waves is possible with an error margin. Trim and sinkage on ships in calm water have minimal impact on air cavity when compared to experimental results. The use of ideal gas versus constant density gas also showed minimal differences. Ideal gas produces angles that are systematically lower than comparable constant density gas with results closer to experiments. This indicates a transverse expansion of bubble cavity. The differences however are minimal with none exceed 4%. Constant density gas was thus used for wave studies.

Trim fluctuation was used to determine one wave cycle in which results can be sampled. The last complete sine curve before injection and first complete sine curve after stable injection marks out the sampling range for simulations with head waves. The maximum transverse position of air cavities and their corresponding sweep angles were drawn at 0.1s interval over wave period (between 1.3s and 1.5s). Drag reduction for calm water was calculated using 1 cycle of fluctuations observed in drag plots before injection and after injection has stabilised. Drag reduction for waves were calculated using the same trim fluctuation cycle for sweep angle calculations. Percentage drag reduction was calculated using Equation 1. Table 5 summarises the sweep angles and drag reduction observed.

$$\%DR = (1 - \frac{Drag_{air\,flux}}{Drag_{no\,air\,flux}}) \times 100\% \tag{1}$$

Freestream Velocity (Fr)	Wave	Air Flux (m^3s^{-1})	Min. Sweep Angle	Max. Sweep Angle	Mean Sweep Angle	% Drag Reduction
$1.647ms^{-1}$ (0.1949)	Calm	2×10^{-5}	-	-	75.13°	5.10%
		2.5×10^{-3}	-	-	73.03°	4.40%
	H_W = 0.6m	2×10^{-3}	71.66°	76.47°	74.37°	9.96%
		2.5×10^{-3}	71.73°	73.47°	72.48°	9.89%
	H_W = 0.12m	2×10^{-3}	72.93°	74.96°	74.10°	11.74%
		2.5×10^{-3}	72.12°	75.66°	73.76°	11.58%
$1.922ms^{-1}$ (0.2274)	Calm	2×10^{-5}	-	-	78.32°	4.91%
		2.5×10^{-3}	-	-	78.30°	2.61%
	H_W = 0.6m	2×10^{-3}	76.91°	80.56°	78.18°	11.76%
		2.5×10^{-3}	75.71°	77.34°	76.60°	11.08%
	H_W = 0.12m	2×10^{-3}	77.96°	79.35°	78.70°	4.58%
		2.5×10^{-3}	77.10°	78.49°	77.95°	4.03%
$2.196ms^{-1}$ (0.2599)	Calm	2×10^{-5}	-	-	80.05°	3.50%
		2.5×10^{-3}	-	-	79.54°	3.11%
	H_W = 0.6m	2×10^{-3}	77.75°	81.84°	80.28°	3.74%
		2.5×10^{-3}	78.21°	80.86°	79.29°	3.43%
	H_W = 0.12m	2×10^{-3}	78.32°	81.42°	79.48°	6.3%
		2.5×10^{-3}	77.36°	80.46°	78.62°	5.75%

Table 5: Different observed sweep angles and drag reduction

An increase in freestream velocity tends to increase the sweep angle made by air cavity. The resulting sharper form and the lowering of air layer coverage explains the general drop in drag reduction observed. Wave height and the corresponding change in ship's trim and sinkage does not appear to affect sweep angle as much. The slightly lower mean sweep angle and drag reduction suggests ALS can still work in non-calm waters. However, it should not be an indication that voyage across rough seas can offer better economics due to higher percentage drag reduction. In multiple cases, an increase in air flux results in decreasing φ, suggesting greater air coverage. The contrasting decrease in drag reduction may stem from higher injection speed causing cavity to interact with ship hull further downstream as buoyancy needs a longer time to overcome downwards momentum from injection.

4 Conclusions and Ongoing Work

A limitation of CFD code used is the need for VoF model to be utilised to generate waves. VoF model is able to resolve flow cavity but with error of up to 6.45%. The use of ideal gas improves the accuracy of sweep angle resolved by approximately 1-2%. Ideal gas use will however induce an increase in numerical instability and computation cost, especially for simulations in head waves. The assumption of gas having constant density is thus recommended.

Head waves affect how air cavity form on flat bottom of ships. Height of waves have less impact on air cavity than freestream velocity. Drag reduction can be observed in all cases with air injection, even when waves are present. A proper calibration of flux and freestream velocity should result in significant drag reduction.

Cavities in oblique waves and lagrangian tracking of bubbles are ongoing.

References

[1] International Towing Tank Confernce. Practical guidelines for ship resistance CFD.

[2] Hee-Taek Kim, Hyoung-Tae Kim, Jung-Joong Kim, and Dong-Yeon Lee. Study on the skin-friction drag reduction by air injection using computational fluid dynamics-based simulations. 56(4):20.

[3] Simo A. Mäkiharju, In-Ho R. Lee, Grzegorz P. Filip, Kevin J. Maki, and Steven L. Ceccio. The topology of gas jets injected beneath a surface and subject to liquid cross-flow. 818:141–183.